Photoresponsive block copolymer nanostructures through implementation of arylazopyrazoles

Katharina Ziegler, Lisa Schlichter, Yorick Post, André H. Gröschel, Bart Jan Ravoo*

K. Ziegler, L. Schlichter, Y. Post, B. J. Ravoo: Organic Chemistry Institute and Center for Soft Nanoscience, University of Münster, Corrensstraße 40, 48149 Münster, Germany, E-mail: b.j.ravoo@uni-muenster.de

A. H. Gröschel: Bavarian Center for Battery Technology (BayBatt) and Bavarian Polymer Institute (BPI), University of Bayreuth, Universitätsstraße 30, 95448 Bayreuth, Germany

KEYWORDS. block copolymers, molecular photoswitches, responsive materials, self-assembly

ABSTRACT: Responsive nanomaterials that can undergo reversible changes in morphology are interesting for the development of functional materials that interact with and respond to their environment. Amphiphilic block copolymers are well-known for their ability to create a wide range of supramolecular nanostructures in solution. Arylazopyrazoles (AAPs) are versatile molecular photoswitches, which change their configuration and hydrophobicity via irradiation with UV light (365 nm, Z isomer, less hydrophobic) and green light (520 nm, E isomer, more hydrophobic). In this work, photoswitchable block copolymers containing arylazopyrazole tetraethylene glycol methacrylate (AAPMA) and oligo(ethylene glycol) methacrylate (OEGMA) forming amphiphilic POEGMA-b-PAAPMA with varying block lengths are prepared by RAFT polymerization. The photochemical properties of AAP persist in the polymers. Due to their amphiphilic structure, the polymers self-assemble into supramolecular morphologies in water. Remarkably, photoisomerization results in a reversible change in the self-assembly behavior. Specifically, spherical and cylindrical micelles are observed for POEGMA33-b-PAAPMA47 when illuminated under green or UV light during assembly. Furthermore, the morphology of assembled structures can be reversibly switched by subsequent irradiation with UV and green light.

Introduction

Supramolecular structures that can undergo a reversible shape transformation are of great interest for the development of intelligent materials[1,2] and drug delivery approaches.[3–6] In particular, block copolymers (BCPs) are capable of creating a diverse array of nanostructures.[7–9] BCPs consist of two or more covalently-linked segments, whose chemical incompatibility results in microphase separation. Furthermore, driven by a difference in solubility, they are capable of forming a variety of supramolecular nanostructures in solution.[10,11] Shape and morphology of these nanostructures strongly depends on volume fractions of the different blocks and can be approximated by the packing parameter as defined for surfactants.[12]

Response to external stimuli is essential for implementing morphological transitions into polymeric systems.[13,14] Among others, reduction and oxidation,[15,16] pH[17,18], and temperature[19,20] have been implemented as external triggers for responsive BCPs. Light is a very attractive stimulus, owing to its high temporal and spatial resolution, as well as the possibility to apply it externally. Most often, photoresponse is achieved by switching between two isomers of a molecular photoswitch through a reversible photoisomerization upon irradiation with light of a certain wavelength.[21–25] A well-studied example is the photoswitch azobenzene which has been implemented in various photoresponsive BCPs.[26–29] The related arylazopyrazoles (AAPs) have not yet been integrated in BCPs, despite their unique photophysical properties. Compared to azobenzene, AAPs show high photostationary states (PSS) and long thermal half-lives of the metastable *Z* isomer.[23,30,31] Upon irradiation with UV light, AAPs undergo a change in configuration to the bent *Z* isomer, which has an increased dipole moment and a lower hydrophobicity as compared to the linear *E* isomer.[32]

Many photoresponsive BCPs exhibit a shape transition in the solid state[33–35] or their transitions in solution are based on supramolecular interactions, such as host-guest complexes.[36–39] In comparison, less examples exist on the self-assembly of BCPs with photoresponsive blocks in solution. In one prominent example, Wang *et al.* studied an alternating azo copolymer that can undergo a photoinduced deformation.[40] The amphiphilic epoxy-based alternating azo copolymer can assemble in water into colloidal spheres which deform into ellipsoids under irradiation with an Ar^+ laser at 488 nm. It has also been reported that assembled alternating copolymers or BCP structures containing azobenzene can be disassembled and reassembled by irradiation.[28,41–44]

In this study, we report AAP-bearing amphiphilic BCPs capable of forming different assemblies in solution upon photoisomerization of the AAP. To this end, a library of different amphiphilic poly(oligo(ethylene glycol) methacrylate-*block*-poly(arylazopyrazole tetra(ethylene glycol) methacrylate) (POEGMA-*b*-PAAPMA) was synthesized with AAPs incorporated into the hydrophobic block. The configuration of the AAP can be altered by green light (520 nm, *E* isomer) and UV light (365 nm, *Z* isomer). As result of this configuration change, the hydrophobicity of the AAP-bearing block changes, in turn affecting the morphology

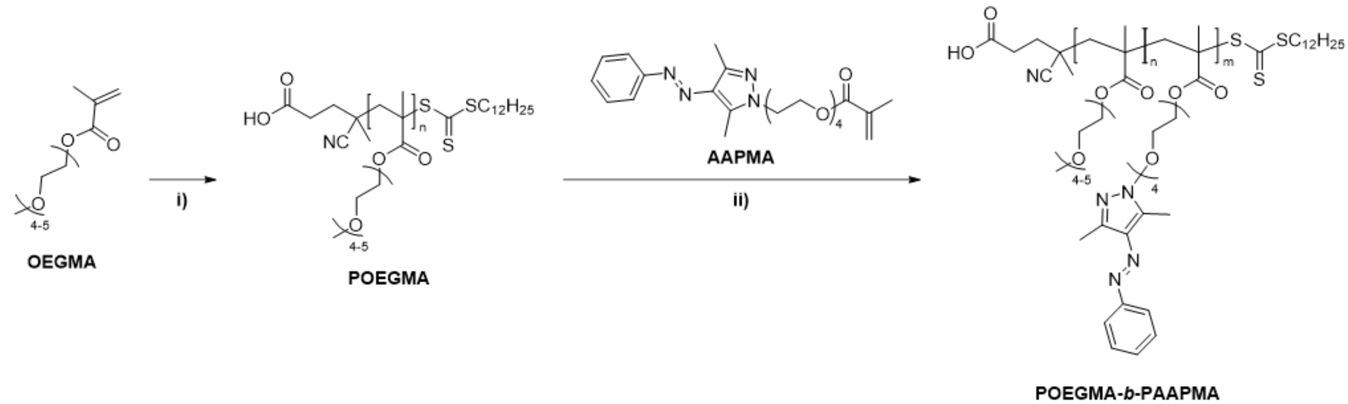

Scheme 1. Synthesis of POEGMA-*b*-PAAPMA. i): RAFT polymerization of OEGMA using CDPA as chain transfer agent (CTA), AIBN, dioxane, 70 °C, 3 h to 6 h. ii): Block copolymerization using the photoswitchable AAPMA monomer, AIBN, DMF, 70 °C, 3 h to 6 h. Variation of the reaction time leads to different block lengths.

of the BCP micelles. Consequently, the assembly behavior of POEGMA-*b*-PAAPMA can be controlled externally by inducing photoisomerization.

Results and Discussions

Amphiphilic POEGMA-*b*-PAAPMAs with varying block lengths were synthesized *via* reversible addition-fragmentation chain-transfer (RAFT) polymerization (**Scheme 1**). The monomer OEGMA with an molecular weight M_n = 300 g/mol was polymerized using 4-cyano-4-(((dodecylthio)carbonothioyl)thio)pentanoic acid (CDPA), a commercially available chain transfer agent (CTA) that is suitable for more activated monomers such as methacrylates[45,46], and AIBN as radical initiator. POEGMA was synthesized in three different block lengths of 33, 41 and 66 to achieve different morphologies of the BCPs. The monomer AAPMA for the second block contains AAP as photoswitchable unit linked to a methacrylate moiety. Due to the hydrophobic character of *E*-AAP, it is the counterpart of the hydrophilic OEGMA and forms the main part of the hydrophobic block. Furthermore, the photoswitch can undergo reversible *E-Z* isomerization using UV and green light, which is the key element for achieving the desired morphological change at the nanoscale. The methacrylate unit is necessary to ensure compatibility of AAPMA with CDPA. A tetraethylene glycol (TEG) linker was implemented between the AAP side group and the methacrylate backbone to ensure photoisomerization is not sterically hindered (synthesis procedures see Supplementary Information S4, NMR spectra **Figures S1-S2**).

In a second polymerization step, the previously synthesized POEGMAs were used as macro-CTA and POEGMA-*b*-PAAPMA polymers with varying block lengths were synthesized to have a wide range of POEGMA weight fractions. The polymers contain varying amounts of photoswitch to investigate the impact of AAP in the polymers. The block length and dispersity were determined using gel permeation chromatography (GPC) (**Table 1, Figure S3**). Six distinct BCPs were obtained with molecular weights (M_n) ranging from 16500 g/mol to 62400 g/mol. All polymers are well-defined as shown by narrow GPC traces and dispersities ranging from 1.30 to 1.51. The weight fractions range from $f_{hydrophilic}$ = 0.16, where the polymer is dominated by the photoswitchable block, to 0.60, where the hydrophilic POEGMA block is twice as long as the hydrophobic PAAPMA.

Table 1 Properties of POEGMA-*b*-PAAPMA. Degree of polymerization (DP) of POEGMA and PAAPMA blocks determined by ^{1}H NMR spectroscopy, molecular weight (M_n) of POEGMA b PAAPMA determined by GPC, weight fraction of the hydrophilic block ($f_{hydrophilic}$), dispersity (Đ) and assembled structures observed in transmission electron microscopy (TEM) after irradiation with UV light (365 nm) or green light (520 nm).

BCP	DP POEGMA	DP PAAPMA	M_n [g/mol] BCP	$f_{hydrophilic}$	*Đ*	Micelle morphology 365 nm / 520 nm
P1	33	14	16 500	0.60	1.30	spherical / spherical
P2	33	47	31 200	0.32	1.31	cylindrical / spherical
P3	33	73	42 700	0.23	1.30	spherical / undefined
P4	33	115	62 400	0.16	1.42	spherical / undefined
P5	41	52	35 500	0.34	1.42	spherical / spherical
P6	66	53	43 700	0.45	1.51	spherical / spherical

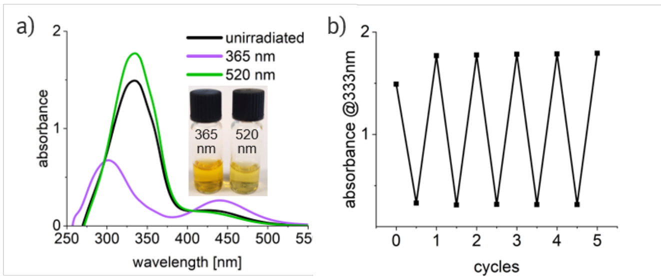

Figure 1. Photoisomerization of **P2** in water (0.05 mg/mL) at room temperature. a) UV-vis spectra demonstrating photoswitching of AAP in **P2**, unirradiated and after 5 min irradiation with UV (365 nm) and green light (520 nm), inset shows the color change. b) Reversible photoswitching over five cycles.

The photoisomerization of PAAPMA can be seen by the naked eye due to a color change. Upon illumination of an aqueous POEGMA-*b*-PAAPMA solution, the solution changes from yellow to orange (UV light, 365 nm) and back to yellow (green light, 520 nm). The photophysical properties of all polymers were analyzed using UV-vis spectroscopy (**Figure 1a, S4-S8**). Aqueous polymer solutions were measured before and after irradiating for 2 min with UV light and 5 min with green light to monitor the photoisomerization.

The initial spectrum of **P2** shows a maximum at 333 nm corresponding to the π-π^* transition (**Figure 1b)**. Irradiation with UV light leads to a characteristic hypsochromic shift and an intensity decrease for the π-π^* band, accompanied by an increase in intensity of the n-π^* band at 450 nm. Back isomerization was achieved by irradiation with green light. This behavior is reversible for at least five cycles. All polymers show similar results **(Figures S4-S8**). It can be concluded that the integration of AAP into the PAAPMA does not prevent photoisomerization.

Understanding the thermal stability and corresponding half-life ($t_{1/2}$) of the *Z* isomer in the polymers is crucial for the assembly process into nanostructures. If $t_{1/2}$ is short, the assembly process must be carried out under permanent irradiation, which can cause temperature increases and consequently affect the assembly process. For longer $t_{1/2}$, the samples can be irradiated beforehand and assembled in a dark environment, resulting in better controllability. The thermal *Z-E* isomerization for **P2** in aqueous solution was monitored by UV-vis spectroscopy at 60 °C, 70 °C, and 80 °C (**Figures S9-S11**), to determine the *Z* isomer half-life in the polymer. The data was extrapolated using a linearized Eyring equation[47] to calculate the half-life to $t_{1/2,\ 25\ °C}$ = 110 h (**Figure S12**). The thermal stability is of similar magnitude to monomeric AAPMA ($t_{1/2,\ 25\ °C}$ = 75 h, **Figure S13-S16**).

BCPs can spontaneously self-assemble when they have two or more chemically incompatible segments. Self-assembly in solution is driven by a sufficient difference in solubility of each block.[48] The assembly protocol plays a crucial role in controlling the process and the resulting nanostructures.[49] A two-step assembly method I (see **Figure S17**) was utilized as an established nanoprecipitation method.[50] After dissolving POEGMA-*b*-PAAPMA in DMF (1 mg/mL, completely dissolving the BCP), the sample was irradiated with either UV (2 min) or green light (5 min) to ensure conversion to *E*-PAAPMA or *Z*-PAAPMA, respectively. Subsequently, the solution was slowly injected into water with an addition rate of 1.9 ml/h for 2 h until a ratio of 4:1 (H_2O:DMF) was reached. Then, DMF was slowly exchanged with water within 1.5 days *via* dialysis. The assembly process was carried out in dark conditions and irradiation was occasionally repeated to ensure the targeted isomer was maintained during the process.

The polymers **P1** and **P3-P6** assembled into spherical micellar structures as analyzed by dynamic light scattering (DLS) and transmission electron microscopy (TEM) (**Table 1**, **Figures S18-S26**). Here, the water-soluble POEGMA block forms the corona, while the hydrophobic PAAPMA forms the core of the micelles. Most interestingly, different morphologies were observed in DLS and TEM for **P2** when assembled under UV light and green light (**Figure 3**).

A first indication that the self-assembly behavior changes for the photo-isomers of the PAAPMA block in **P2** is the change of hydrodynamic diameter (d_h) obtained from DLS. For the *Z* isomer, a d_h = 137 nm was observed which was significantly higher than for the *E* isomer (d_h = 81 nm) (**Figure 2a**). Further investigation using angle-dependent DLS revealed more detail about the assembled structures. For spherical particles, a linear relationship between the relaxation rate Γ and the squared scattering vector q^2 is expected.[51] Nonlinear angular behavior arises for samples with anisotropic shapes and high flexibility, such as cylindrical micelles.[52] To emphasize the angular scattering behavior, the apparent diffusion constant Γ/q^2 was plotted as a function of q^2. **Figure 2b** shows linear behavior for the *E* isomer, neglecting low angles, where laser afterpulsing and hardware errors are increased. This confirms the presence of spherical objects. In contrast, the assemblies obtained from the *Z* isomer showed an increase at low scattering vectors, which levels off at higher q^2 and are a first indication of cylindrical micelles. Conclusively, TEM images revealed that **P2** with *Z* AAP assembles into cylindrical structures with a diameter of 34 ± 4 nm and a length in the µm range (**Figure 2c**). In contrast, **P2** containing *E* AAP assembles into spherical micellar structures with diameters of 64 ± 21 nm (**Figure 2d**, **Figure S24**).

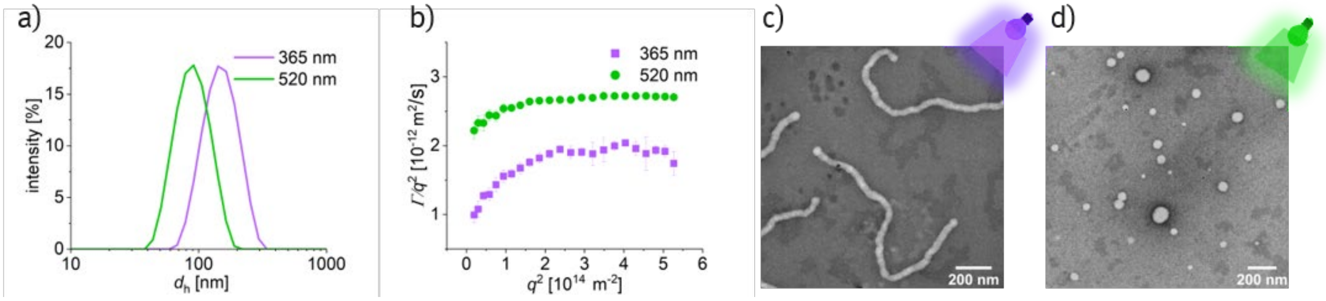

Figure 2. Analysis of **P2** assemblies in water at room temperature prepared by assembly method I. a) Size distributions of the assemblies as determined by DLS. b) Angle-dependent DLS measurements of the assemblies. c) TEM image of the morphologies obtained for the *Z* isomer. d) TEM image of the morphologies obtained for the *E* isomer.

The self-assembly of BCP into spherical or cylindrical micelles is determined by the relative volume fractions of corona and core. The range of volume fractions, and additionally the assembly conditions, in which cylindrical micelles are formed can be very specific.[53] Apparently, **P2** hits this sweet spot where a small change in relative volume fractions caused by the photoisomerization of the AAP block leads to different morphologies. For other polymers (**P1** and **P3-P6**), no such pronounced structural effect was observed. The structural change of **P2** assemblies is not yet fully understood. It may be expected that the photoisomerization of AAP changes the balance of intermolecular interactions of the BCP in aqueous solution. The *E* isomer has a planar structure and tends to π-π stacking, while the *Z* isomer has a twisted structure where such interactions are not possible.[54] Reduced self-interaction may affect the packing of the AAP block. Furthermore, photoisomerization from *E* to *Z* leads to an increase in dipole moment and a decrease in hydrophobicity of the AAP block.[32] Based on a simple packing parameter analysis in analogy to low molecular weight surfactants, spherical micelles for the more hydrophilic *Z* isomer and cylindrical micelles for the more hydrophobic *E* isomer would be predicted, but we consistently observe the opposite. Hence, it would appear that the assembly of **P2** is affected by stronger hydration and swelling of the *Z* AAP in the BCP micelle core, leading to a destabilization of the spherical micelles and transition into cylindrical micelles.

Next, the ability to photoswitch between spherical and cylindrical micelles after assembly was analyzed. Mild conditions were chosen to assemble **P2** (assembly method II, see **Figure S27**). The polymer was dissolved in DMF (1 mg/mL), irradiated with UV or green light, and subsequently dialyzed against water. The resulting nanostructures for assembly method II are similar to the ones observed for assembly method I. TEM measurements revealed cylindrical micelles with diameters of 32 ± 4 nm and lengths in the µm-range when assembled under UV light. In contrast, green light led to spherical micelles with diameters ranging from 35 nm to 277 nm with an average value of 105 ± 49 nm, which is larger than for the first batch (64 ± 21 nm) (**Figure 3a i and ii**, **Figure S25**).

Differential scanning calorimetry (DSC) was performed to determine the glass transition temperature of the unirradiated **P2** containing mainly *E* isomer. The *Z* isomer cannot be measured by DSC, as the high temperatures inherent in the measurement significantly shorten its half-life. DSC shows that **P2** exhibits a single glass transition below 0 °C

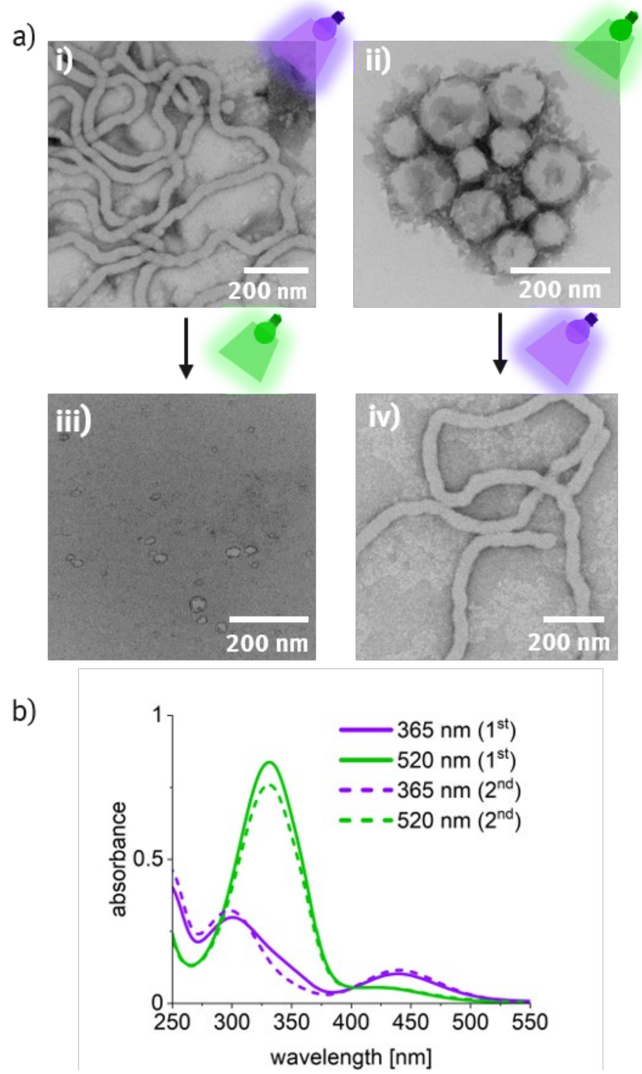

Figure 3. Molecular and structural photoswitching after assembly of **P2** in water using assembly method II. a) TEM images after irradiation in DMF and assembly via dialysis (i, ii) and after irradiation of the assemblies in aqueous solution for 1 h with green (520 nm, iii) or UV light (365 nm, iv). b) UV-vis spectra of assembled micelle solutions (365 nm and 520 nm 1st). Dotted lines indicate spectra after irradiation (5 min) of pre-prepared assemblies with green light (520 nm 2nd) or UV light (365 nm 2nd).

(**Figure S28**). This observation indicates that the polymer has sufficient chain mobility to enable structural transformations at room temperature. Next, the cylindrical micelles, consisting of the *Z* isomer, were irradiated with green light and the spherical *E* isomer micelles, were irradiated with UV light. UV-vis measurements indicated complete *E*-*Z* isomerization and almost complete *Z*-*E* isomerization after 5 min of irradiation (**Figure 3b**).

Photoisomerization occurs rapidly within 5 min on a molecular level. To ensure that the BCP has sufficient time to transform, we irradiated the structures for longer times. After 1 h, a shape transformation was observed in TEM imaging for both isomers (**Figure 3a iii and iv**). The cylindrical micelles transformed into spherical micelles with a diameter of 24 ± 12 nm (**Figure S26b**). Conversely, exposure of spherical micelles to UV light resulted in a shape transformation into cylindrical micelles. The assemblies have a diameter of 47 ± 7 nm and a length in the µm-range, similar to the previously observed structures (**Figure S26b)**. These data indicate reversible photoswitching of the BCP at both molecular and structural levels.

Conclusion

In conclusion, the implementation of AAP photoswitches into amphiphilic BCPs has resulted in photoresponsive BCP micelles. We created a library of BCPs with different block length of the hydrophilic and hydrophobic blocks. Integration of the AAP into the polymer did not affect the excellent switching behavior of the photoswitch. **P2** showed that the configuration of AAP affects the relative volume fraction and consequently the aggregation behavior of the polymer. *E* isomer **P2** forms spherical micelles, whereas the *Z* isomer forms cylindrical micelles. Two different assembly methods were used, resulting in similar supramolecular structures. Furthermore, it was demonstrated that the assembled structure can be reversibly transformed into another morphology simply by irradiation with light. This feature makes these responsive BCPs interesting for applications in actuators, intelligent materials, and for drug release.

ASSOCIATED CONTENT

Supporting Information. Materials and Methods, synthesis, ^{1}H NMR spectra, GPC, UV-vis, determination of thermal half-lives, DLS, TEM, DSC.

AUTHOR INFORMATION

Corresponding Author

B. J. Ravoo - Organic Chemistry Institute and Center for Soft Nanoscience, University of Münster, Corrensstraße 40, 48149 Münster, Germany, orcid.org/0000-0003-2202-7485; E-mail: b.j.ravoo@uni-muenster.de.

Authors

K. Ziegler - Organic Chemistry Institute and Center for Soft Nanoscience, University of Münster, Corrensstraße 40, 48149 Münster, Germany.

L. Schlichter- Organic Chemistry Institute and Center for Soft Nanoscience, University of Münster, Corrensstraße 40, 48149 Münster, Germany.

Y. Post - Organic Chemistry Institute and Center for Soft Nanoscience, University of Münster, Corrensstraße 40, 48149 Münster, Germany.

A. H. Gröschel - Bavarian Center for Battery Technology (BayBatt) and Bavarian Polymer Institute (BPI), University of Bayreuth, Universitätsstraße 30, 95448 Bayreuth, Germany.

Funding Sources

DFG CRC 1459 Intelligent Matter, Project-ID 433682494 and INST 211/719-1 FUGG

Notes

There are no conflicts to declare.

Acknowledgements

The authors would like to thank Debbie Stappers for DSC measurements. This work was funded by the Deutsche Forschungsgesellschaft (DFG CRC 1459 Intelligent Matter, Project-ID 433682494 and INST 211/719-1 FUGG for TEM instrumentation).

References

(1) Kaspar, C.; Ravoo, B. J.; van der Wiel, W. G.; Wegner, S. V.; Pernice, W. H. P. The rise of intelligent matter. Nature 2021, 594 (7863), 345–355. DOI: 10.1038/s41586-021-03453-y.
(2) Walther, A. Viewpoint: From Responsive to Adaptive and Interactive Materials and Materials Systems: A Roadmap. Adv. Mater. 2020, 32 (20), e1905111. DOI: 10.1002/adma.201905111.
(3) Johnson, R. P.; Preman, N. K. Responsive block copolymers for drug delivery applications. Part 1: Endogenous stimuli-responsive drug-release systems. In Stimuli Responsive Polymeric Nanocarriers for Drug Delivery Applications, Volume 1; Elsevier, 2018; pp 171–220. DOI: 10.1016/B978-0-08-101997-9.00009-6.
(4) Johnson, R. P.; Preman, N. K. Responsive block copolymers for drug delivery applications. Part 2: Exogenous stimuli-responsive drug-release systems. In Stimuli Responsive Polymeric Nanocarriers for Drug Delivery Applications, Volume 1; Elsevier, 2018; pp 221–246. DOI: 10.1016/B978-0-08-101997-9.00010-2.
(5) Yin, J.; Chen, Y.; Zhang, Z.-H.; Han, X. Stimuli-Responsive Block Copolymer-Based Assemblies for Cargo Delivery and Theranostic Applications. Polymers 2016, 8 (7). DOI: 10.3390/polym8070268.
(6) Binauld, S.; Stenzel, M. H. Acid-degradable polymers for drug delivery: a decade of innovation. Chem. Commun. 2013, 49 (21), 2082–2102. DOI: 10.1039/c2cc36589h.
(7) Klok, H.-A.; Lecommandoux, S. Supramolecular Materials via Block Copolymer Self-Assembly. Adv. Mater. 2001, 13 (16), 1217. DOI: 10.1002/1521-4095(200108)13:16<1217:AID-ADMA1217>3.0.CO;2-D.
(8) Harada, A.; Kataoka, K. Supramolecular assemblies of block copolymers in aqueous media as nanocontainers relevant to biological applications. Prog. Polym. Sci. 2006, 31 (11), 949–982. DOI: 10.1016/j.progpolymsci.2006.09.004.
(9) Zeng, H.; Roberts, D. A. Recent Progress in Stimuli-Induced Morphology Transformations of Block Copolymer Assemblies. Aust. J. Chem. 2022, 75 (2), 55–64. DOI: 10.1071/CH21200.
(10) Israelachvili, J. N.; Mitchell, D. J.; Ninham, B. W. Theory of self-assembly of hydrocarbon amphiphiles into micelles and bilayers. J. Am. Chem. Soc. 1976, 72, 1525. DOI: 10.1039/f29767201525.
(11) Mai, Y.; Eisenberg, A. Self-assembly of block copolymers. Chem. Soc. Rev. 2012, 41 (18), 5969–5985. DOI: 10.1039/c2cs35115c.

(12) Deng, Z.; Liu, S. Emerging trends in solution self-assembly of block copolymers. Polymer 2020, 207, 122914. DOI: 10.1016/j.polymer.2020.122914.
(13) Idumah, C. I. Multifunctional properties optimization and stimuli-responsivity of shape memory polymeric nanoarchitectures and applications. Polym. Eng. Sci. 2023, 63 (7), 1857–1873. DOI: 10.1002/pen.26331.
(14) Dayyoub, T.; Maksimkin, A. V.; Filippova, O. V.; Tcherdyntsev, V. V.; Telyshev, D. V. Shape Memory Polymers as Smart Materials: A Review. Polymers 2022, 14 (17). DOI: 10.3390/polym14173511.
(15) Liu, L.; Rui, L.; Gao, Y.; Zhang, W. Self-assembly and disassembly of a redox-responsive ferrocene-containing amphiphilic block copolymer for controlled release. Polym. Chem. 2015, 6 (10), 1817–1829. DOI: 10.1039/C4PY01289E.
(16) Feng, A.; Yan, Q.; Zhang, H.; Peng, L.; Yuan, J. Electrochemical redox responsive polymeric micelles formed from amphiphilic supramolecular brushes. Chem. Commun. 2014, 50 (36), 4740–4742. DOI: 10.1039/c4cc00463a.
(17) Kocak, G.; Tuncer, C.; Bütün, V. pH-Responsive polymers. Polym. Chem. 2017, 8 (1), 144–176. DOI: 10.1039/C6PY01872F.
(18) Ray, P.; Kale, N.; Quadir, M. New side chain design for pH-responsive block copolymers for drug delivery. Colloid. Surface. B 2021, 200, 111563. DOI: 10.1016/j.colsurfb.2021.111563.
(19) Kotsuchibashi, Y.; Ebara, M.; Aoyagi, T.; Narain, R. Recent Advances in Dual Temperature Responsive Block Copolymers and Their Potential as Biomedical Applications. Polymers 2016, 8 (11), 380. DOI: 10.3390/polym8110380.
(20) Hunter, S. J.; Armes, S. P. Shape-Shifting Thermoresponsive Block Copolymer Nano-Objects. J. Colloid Interf. Sci. 2023, 634, 906–920. DOI: 10.1016/j.jcis.2022.12.080.
(21) Dürr, H.; Bouas-Laurent, H. Photochromism:Molecules and systems, Rev. ed.; Elsevier, 2003.
(22) Brieke, C.; Rohrbach, F.; Gottschalk, A.; Mayer, G.; Heckel, A. Light-controlled tools. Angew. Chem. Int. Ed. 2012, 51 (34), 8446–8476. DOI: 10.1002/anie.201202134.
(23) Mukherjee, A.; Seyfried, M. D.; Ravoo, B. J. Azoheteroarene and Diazocine Molecular Photoswitches: Self-Assembly, Responsive Materials and Photopharmacology. Angew. Chem. Int. Ed. 2023, 62 (42). DOI: 10.1002/anie.202304437.
(24) Goulet-Hanssens, A.; Eisenreich, F.; Hecht, S. Enlightening Materials with Photoswitches. Adv. Mater. 2020, 32 (20), e1905966. DOI: 10.1002/adma.201905966.
(25) Russew, M.-M.; Hecht, S. Photoswitches: from molecules to materials. Adv. Mater. 2010, 22 (31), 3348–3360. DOI: 10.1002/adma.200904102.
(26) Weis, P.; Wu, S. Light-Switchable Azobenzene-Containing Macromolecules: From UV to Near Infrared. Macromol. Rapid. Comm. 2018, 39 (1). DOI: 10.1002/marc.201700220.
(27) Wang, D.; Wang, X. Amphiphilic azo polymers: Molecular engineering, self-assembly and photoresponsive properties. Prog. Polym. Sci. 2013, 38 (2), 271–301. DOI: 10.1016/j.progpolymsci.2012.07.003.
(28) Zhao, Y.; He, J. Azobenzene-containing block copolymers: the interplay of light and morphology enables new functions. Soft Matter 2009, 5 (14), 2686. DOI: 10.1039/b821589h.
(29) Yu, H.; Kobayashi, T. Photoresponsive block copolymers containing azobenzenes and other chromophores. Molecules 2010, 15 (1), 570–603. DOI: 10.3390/molecules15010570.
(30) Weston, C. E.; Richardson, R. D.; Haycock, P. R.; White, A. J. P.; Fuchter, M. J. Arylazopyrazoles: azoheteroarene photoswitches offering quantitative isomerization and long thermal half-lives. J. Am. Chem. Soc. 2014, 136 (34), 11878–11881. DOI: 10.1021/ja505444d.
(31) Stricker, L.; Fritz, E.-C.; Peterlechner, M.; Doltsinis, N. L.; Ravoo, B. J. Arylazopyrazoles as Light-Responsive Molecular Switches in Cyclodextrin-Based Supramolecular Systems. J. Am. Chem. Soc. 2016, 138 (13), 4547–4554. DOI: 10.1021/jacs.6b00484.
(32) Arndt, N. B.; Schlüter, F.; Böckmann, M.; Adolphs, T.; Arlinghaus, H. F.; Doltsinis, N. L.; Ravoo, B. J. Self-Assembled Monolayers of Arylazopyrazoles on Glass and Silicon Oxide: Photoisomerization and Photoresponsive Wettability. Langmuir 2022, 38 (2), 735–742. DOI: 10.1021/acs.langmuir.1c02651.
(33) Fang, L.; Yan, W.; Chen, S.; Duan, Q.; Herath, M.; Epaarachchi, J.; Liu, Y.; Lu, C. Light and Shape-Memory Polymers: Characterization, Preparation, Stimulation, and Application. Macromol. Mater. Eng. 2023, 308 (12). DOI: 10.1002/mame.202300158.
(34) Lendlein, A.; Jiang, H.; Jünger, O.; Langer, R. Light-induced shape-memory polymers. Nature 2005, 434 (7035), 879–882. DOI: 10.1038/nature03496.
(35) Weng, L.; Ma, M.; Yin, C.; Fei, Z.-X.; Yang, K.-K.; Ross, C. A.; Shi, L.-Y. Synthesis and Self-Assembly of Silicon-Containing Azobenzene Liquid Crystalline Block Copolymers. Macromolecules 2023, 56 (2), 470–479. DOI: 10.1021/acs.macromol.2c02343.
(36) Yao, X.; Li, T.; Wang, J.; Ma, X.; Tian, H. Recent Progress in Photoswitchable Supramolecular Self-Assembling Systems. Adv. Opt. Mater. 2016, 4 (9), 1322–1349. DOI: 10.1002/adom.201600281.
(37) Zhang, X.; Wang, C. Supramolecular amphiphiles. Chem. Soc. Rev. 2011, 40 (1), 94–101. DOI: 10.1039/b919678c.
(38) Appel, E. A.; Biedermann, F.; Rauwald, U.; Jones, S. T.; Zayed, J. M.; Scherman, O. A. Supramolecular cross-linked networks via host-guest complexation with cucurbit8uril. J. Am. Chem. Soc. 2010, 132 (40), 14251–14260. DOI: 10.1021/ja106362w.
(39) Yao, H.; Ning, Y.; Jesson, C. P.; He, J.; Deng, R.; Tian, W.; Armes, S. P. Using Host-Guest Chemistry to Tune the Kinetics of Morphological Transitions Undertaken by Block Copolymer Vesicles. ACS Macro Lett. 2017, 6 (12), 1379–1385. DOI: 10.1021/acsmacrolett.7b00836.
(40) Li, Y.; He, Y.; Tong, X.; Wang, X. Photoinduced deformation of amphiphilic azo polymer colloidal spheres. J. Am. Chem. Soc. 2005, 127 (8), 2402–2403. DOI: 10.1021/ja0424981.
(41) Yadav, S.; Deka, S. R.; Verma, G.; Sharma, A. K.; Kumar, P. Photoresponsive amphiphilic azobenzene–PEG self-assembles to form supramolecular nanostructures for drug delivery applications. RSC Adv. 2016, 6 (10), 8103–8117. DOI: 10.1039/C5RA26658K.
(42) Tong, X.; Wang, G.; Soldera, A.; Zhao, Y. How can azobenzene block copolymer vesicles be dissociated and reformed by light? J. Phys. Chem. B 2005, 109 (43), 20281–20287. DOI: 10.1021/jp0524274.
(43) Liu, Z.; Yao, Y.; Tao, X.; Wei, J.; Lin, S. Helical Self-Assembly of Amphiphilic Chiral Azobenzene Alternating Copolymers. ACS Macro Lett. 2021, 10 (10), 1174–1179. DOI: 10.1021/acsmacrolett.1c00516.
(44) Zhang, Q.; Ko, N. R.; Oh, J. K. Recent advances in stimuli-responsive degradable block copolymer micelles: synthesis and controlled drug delivery applications. Chem. Commun. 2012, 48 (61), 7542–7552. DOI: 10.1039/c2cc32408c.
(45) Keddie, D. J. A guide to the synthesis of block copolymers using reversible-addition fragmentation chain transfer (RAFT) polymerization. Chem. Soc. Rev. 2014, 43 (2), 496–505. DOI: 10.1039/c3cs60290g.
(46) Mayadunne, R. T. A.; Rizzardo, E.; Chiefari, J.; Chong, Y. K.; Moad, G.; Thang, S. H. Living Radical Polymerization with Reversible Addition−Fragmentation Chain Transfer (RAFT Polymerization) Using Dithiocarbamates as Chain Transfer Agents. Macromolecules 1999, 32 (21), 6977–6980. DOI: 10.1021/ma9906837.
(47) Ludwanowski, S.; Ari, M.; Parison, K.; Kalthoum, S.; Straub, P.; Pompe, N.; Weber, S.; Walter, M.; Walther, A. pH Tuning of Water-Soluble Arylazopyrazole Photoswitches. Chem. Eur. J. 2020, 26 (58), 13203–13212. DOI: 10.1002/chem.202000659.
(48) Mai, Y.; Eisenberg, A. Self-assembly of block copolymers. Chem. Soc. Rev. 2012, 41 (18), 5969–5985. DOI: 10.1039/C2CS35115C.
(49) Vena, M. P.; Moor, D. de; Ianiro, A.; Tuinier, R.; Patterson, J. P. Kinetic state diagrams for a highly asymmetric block copolymer

assembled in solution. Soft Matter 2021, 17 (4), 1084–1090. DOI: 10.1039/D0SM01596B.
(50) Silva-Flores, P. G.; Galindo-Rodríguez, S. A.; Pérez-López, L. A.; Álvarez-Román, R. Development of Essential Oil-Loaded Polymeric Nanocapsules as Skin Delivery Systems: Biophysical Parameters and Dermatokinetics Ex Vivo Evaluation. Molecules 2023, 28 (20). DOI: 10.3390/molecules28207142.
(51) Koppel, D. E. Analysis of Macromolecular Polydispersity in Intensity Correlation Spectroscopy: The Method of Cumulants. J. Chem. Phys. 1972, 57 (11), 4814–4820. DOI: 10.1063/1.1678153.

TOC

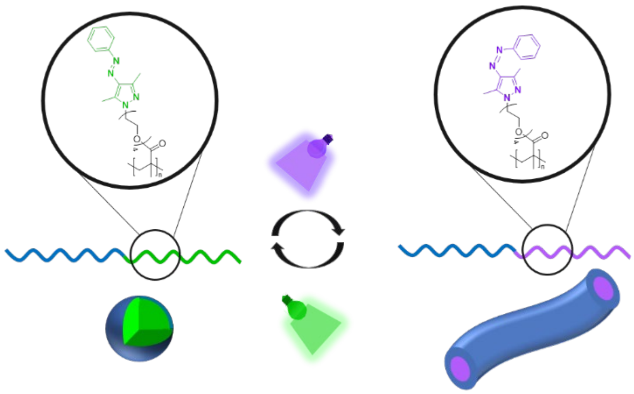

(52) Walther, A.; André, X.; Drechsler, M.; Abetz, V.; Müller, A. H. E. Janus discs. J. Am. Chem. Soc. 2007, 129 (19), 6187–6198. DOI: 10.1021/ja068153v.
(53) Liaw, C. Y.; Henderson, K. J.; Burghardt, W. R.; Wang, J.; Shull, K. R. Micellar Morphologies of Block Copolymer Solutions near the Sphere/Cylinder Transition. Macromolecules 2015, 48 (1), 173–183. DOI: 10.1021/ma501763x.
(54) Chu, C.-W.; Stricker, L.; Kirse, T. M.; Hayduk, M.; Ravoo, B. J. Light-Responsive Arylazopyrazole Gelators: From Organic to Aqueous Media and from Supramolecular to Dynamic Covalent Chemistry. Chem. Eur. J. 2019, 25 (24), 6131–6140. DOI: 10.1002/chem.201806042.